



Enhanced solid-state electrolytes made of lithium phosphorous oxynitride films

J.F. Ribeiro ^{a,*}, R. Sousa ^a, J.P. Carmo ^a, L.M. Gonçalves ^a, M.F. Silva ^a, M.M. Silva ^b, J.H. Correia ^a

^a University of Minho, Dept Industrial Electronics, Campus Azurem, 4800-058 Guimaraes, Portugal

^b University of Minho, Chemistry Centre, Braga, Portugal

ARTICLE INFO

Article history:

Received 18 February 2012

Received in revised form 30 August 2012

Accepted 4 September 2012

Available online 11 September 2012

Keywords:

Film battery

Lithium batteries

Integrated batteries

Materials technology

ABSTRACT

This paper presents glassy films of lithium phosphorus oxynitride electrolyte with an amorphous structure and improved ionic conductivity suitable for solid-state batteries. The films of lithium phosphorus oxynitride electrolyte were obtained by deposition using the RF sputtering technique in a reactive N₂ atmosphere. The measurements showed films with ionic conductivities in range of 10⁻⁷–10⁻⁶ S·cm⁻¹, for temperatures between 22 °C and 43 °C. The depositions were done at several pressures (0.03 Pa, 0.7 Pa and 1 Pa) and for RF applied powers of 150 W and 200 W, in order to evaluate the best deposition set-point. The highest ionic conductivity of 10⁻⁶ S·cm⁻¹ was measured under a practical room temperature of 35 °C on the best films. These results are comparable with the related state-of-the-art.

© 2012 Elsevier B.V. All rights reserved.

1. Introduction

In modern batteries, the selection and characterization of materials as well as film deposition techniques play an important role because the battery performance, durability and reproducibility must be maximized [1]. In this context, electrolytes made of solid-state materials are required to have high ionic conductivity, a negligible electrical conductivity and be stable in contact with the anode and cathode electrodes [2]. These requirements are met with lithium phosphorous oxynitride (LiPON) as the electrolyte material [3,4]. The lithium phosphorous oxynitride is a lithiated glass with a widespread use as electrolyte material, mainly due to the exceptional electrochemical stability and very good conductivity of lithium ions (the ionic conductivity). Since an electronic resistivity higher than 10¹⁴ Ω·cm is a common feature of lithium phosphorous oxynitride films, batteries with increased lifetimes due to the minimization of short circuit self-discharge can be fabricated [5]. The nature of LiPON conductivity is discussed by Kim and Wadley [6], where it was suggested that the conductivity of LiPON does not depend on the N content, but on the deposition conditions. Bates et al. in [7,8] suggest that the highest conductivity for a LiPON film deposited by RF magnetron was based on Li_{2.9}PO_{3.3}N_{0.46}. S. Zhao et al. [9] also reported LiPON films fabricated by pulsed laser

deposition and some research groups attempted to attach LiPON to another materials [10–12]. LiPON ionic conductivity and its relationship to N content are still not fully understood [13]. This paper presents RF sputtered amorphous structured lithium phosphorous oxynitride films, as well as dependence on deposition parameters. These lithium phosphorous oxynitride films are for use as electrolyte in film silicon compatible batteries with structures similar to the one presented in Fig. 1 (representing a film battery fabricated by successive layer deposition on top of a silicon substrate).

2. Lithium phosphorus oxynitride films deposition

The lithium phosphorous oxynitride films presented in this paper were obtained by RF sputtering of lithium phosphate (Li₃PO₄) targets in 20 sccm reactive nitrogen (N₂) plasmas. The RF frequency of the power source was 13.56 MHz with powers of 150 W and 200 W, with a deposition rate from 0.4 Å s⁻¹ to 2.5 Å s⁻¹. The thickness of the films was settled to be 1 μm. The pressure inside the vacuum chamber takes one of the following values: 0.03 Pa, 0.7 Pa and 1 Pa. Table 1 lists the pressure and RF power conditions used during the depositions.

3. Lithium phosphorus oxynitride film characterization

The best batteries are those with the highest ionic conductivity and electrical resistance, because the self-discharge current and the

* Corresponding author. Tel.: +351 253 510190; fax: +351 253 510189.

E-mail address: jribeiro@dei.uminho.pt (J.F. Ribeiro).

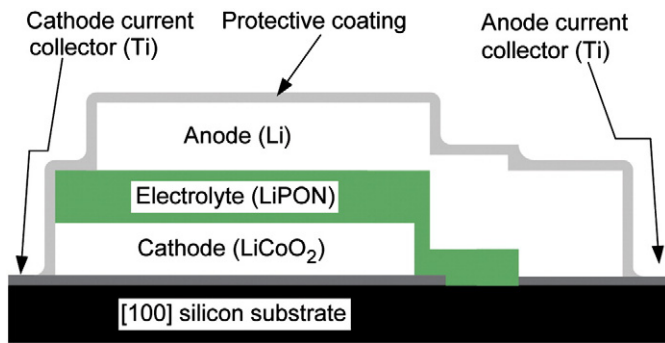


Fig. 1. An artwork of film battery with a solid-state electrolyte made of lithium-phosphorus oxynitride (LiPON). It must be noted that the thickness of each layer is not on scale for better visualization.

Li⁺ conductivity must be minimized and maximized, respectively. It's a well-known and accepted fact that the best electrolyte properties are found on amorphous (the absence of any crystalline structure) materials [14]. In this context, the amorphous materials will result in films with high ionic conduction as compared with crystalline structures. The ionic conductivity was measured on the best samples of lithium phosphorous oxynitride films, following a procedure similarly used by Lee et al. [10] and by Park et al. [15]. The impedance of the selected sample was measured at several frequencies that ranged from 0.5 Hz to 65 kHz with the help of a sinusoidal signal with an amplitude of 12.5 mV. Fig. 2a) shows a photograph of a lithium phosphorous oxynitride sample with contacts of aluminum (Al) and platinum (Pt) for measuring the ionic conductivity. In order to get measurements with high quality and low errors, two platinum (Pt) contacts were deposited by E-Beam on the top and bottom of the LiPON films. The preparing steps of the samples for ionic conductivity measurement are illustrated in Fig. 2b). The first step (i) consists the deposition of a Pt layer on a substrate made of Al for improving the Al/LiPON adhesion and avoiding direct contact of Al to LiPON that could modify properties of the LiPON films. This Al layer also serves as a physical support for the LiPON sample. Then, (ii) the LiPON film is deposited on top of the Pt layer, under the conditions described in this paper. In the third step (iii), a second Pt layer is deposited above the LiPON film for providing the second contact. The second contact is obtained (iv) by gluing the second Pt layer to a second substrate made of aluminum. Glue made of silver (Ag) provides both the mechanical adhesion of Al and Pt, and a second LiPON/Al contact with the smallest electric resistance. It must be noted that the diameter of the second Pt layer is smaller than the diameter of the LiPON to avoid short-circuits between the two Pt layers. Finally, the measurements are taken in the fifth step (v) with the use of lateral needles, responsible for establishing the electric contacts between the

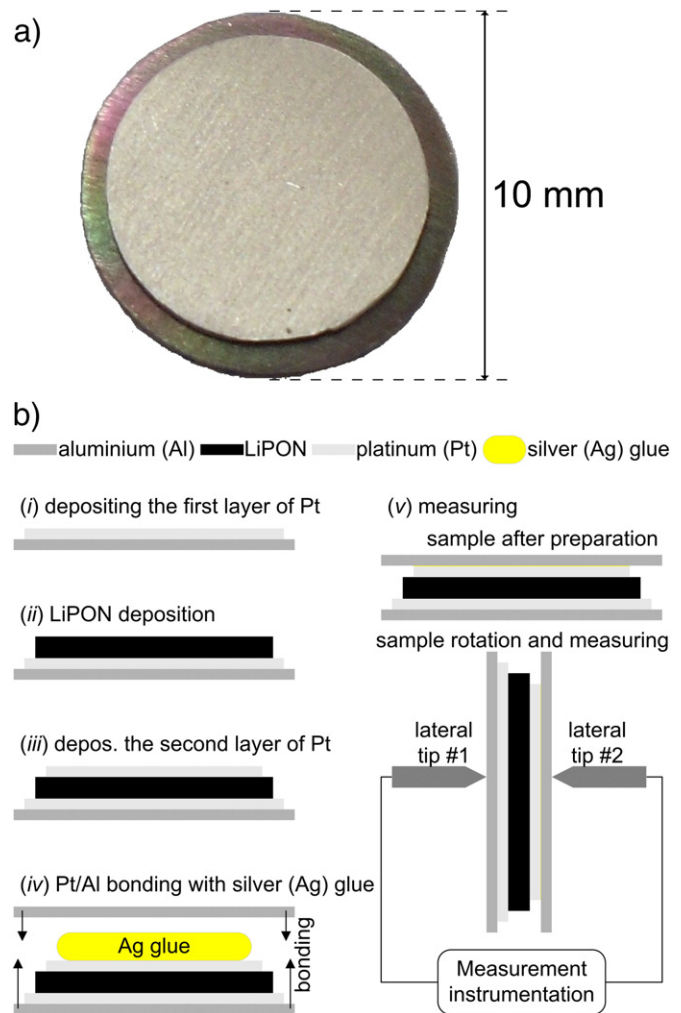


Fig. 2. a) A sample of the LiPON film with top and bottom contacts for ionic conductivity measurement. b) Artwork showing the steps used in the preparation and characterization of the LiPON films.

LiPON sample and the measurement instrumentation. The temperature of the samples during the measurements was controlled using a Büchi TO-50 and the air maintained inert using a glovebox with argon (Ar)

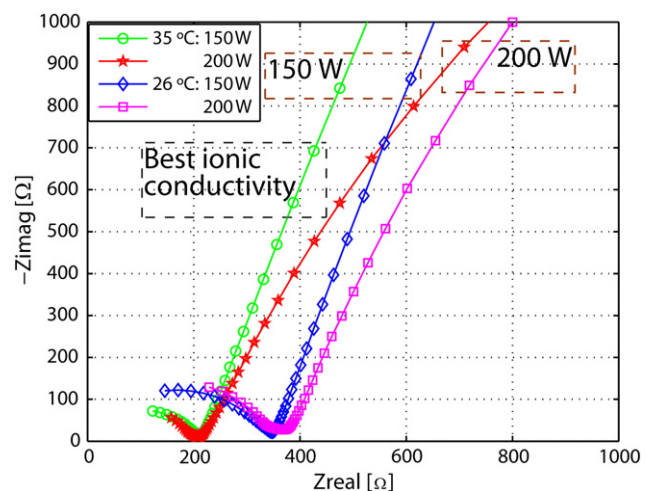


Fig. 3. Nyquist (impedance) diagrams of the LiPON films, deposited at nitrogen (N₂) pressure of 0.03 Pa, RF power of 150 W and 200 W and measured at temperatures of 26 °C and 35 °C.

Table 1

Parameters during the solid-state electrolyte depositions made of LiPON and the best ionic conductivity measured at a room temperature of 35 °C.

Film	Target	N ₂ [sccm]	RF power [W]	Pressure [Pa]	Dep. rate [Å s ⁻¹]	Ionic conductivity [S·cm ⁻¹]
1	Li ₃ PO ₄	20	150	0.03	0.4	10 ⁻⁶
2			200		1.1	6.3 × 10 ⁻⁷
3				0.7	1.9	3.1 × 10 ⁻⁷
4				1	2.5	2.5 × 10 ⁻⁸

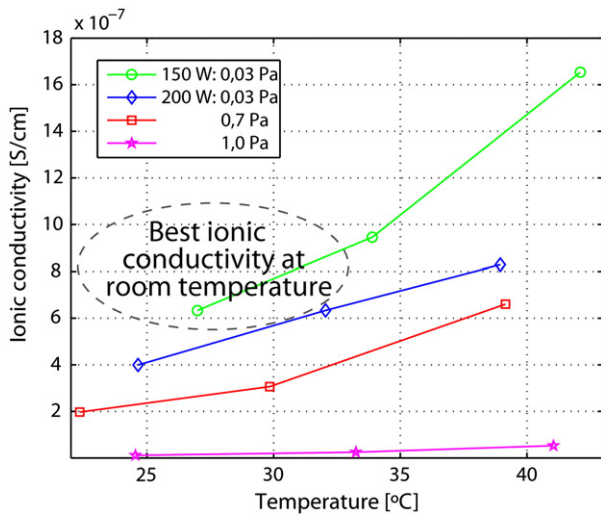


Fig. 4. Ionic conductivity of LiPON deposited with RF power of 150 W (with N₂ pressure of 0.03 Pa) and 200 W (with N₂ pressures of 0.03, 0.7 and 1 Pa) and measured in the temperature range of 22–43 °C.

atmosphere. In this context, after doing the deposition of platinum contacts, the next step was to render respectively, a plot with the both real, Z_{real} , and imaginary, $-Z_{imag}$, parts of the measured impedances in x -axis and y -axis in order to obtain a two-dimensional Nyquist diagram. The Nyquist plots in Fig. 3 are for the samples deposited at N₂ pressures of 0.03 Pa and 0.7 Pa, with RF sputtering powers of 150 W and 200 W. The measurements were taken at 26 °C and 35 °C. In these plots, the diameter of each semi-circle indicates the resistance, R [Ω], of the respective lithium phosphorous oxynitride film (obtained in Autolab software). The highest ionic conductivity was measured for the sample deposited with a pressure of 0.03 Pa, with a temperature of 35 °C and RF power of 150 W. For these conditions, the best ionic conductivity was measured to be located between 10^{-7} S·cm⁻¹ and 10^{-6} S·cm⁻¹ (see Fig. 4). The ionic conductivity is strongly dependent with temperature, that was also measured for room temperatures between 22 °C and 43 °C for the following combinations of deposition parameters in order to evaluate the best sputtering set-point: N₂ pressures of 0.03 Pa (with powers of 150 W and 200 W), 0.7 Pa (200 W) and

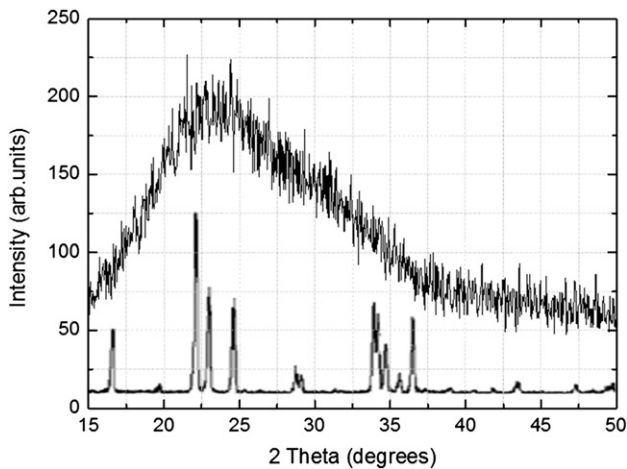


Fig. 5. X-ray diffraction patterns of the LiPON film (top line) and the Li₃PO₄ sputtering target (bottom line).

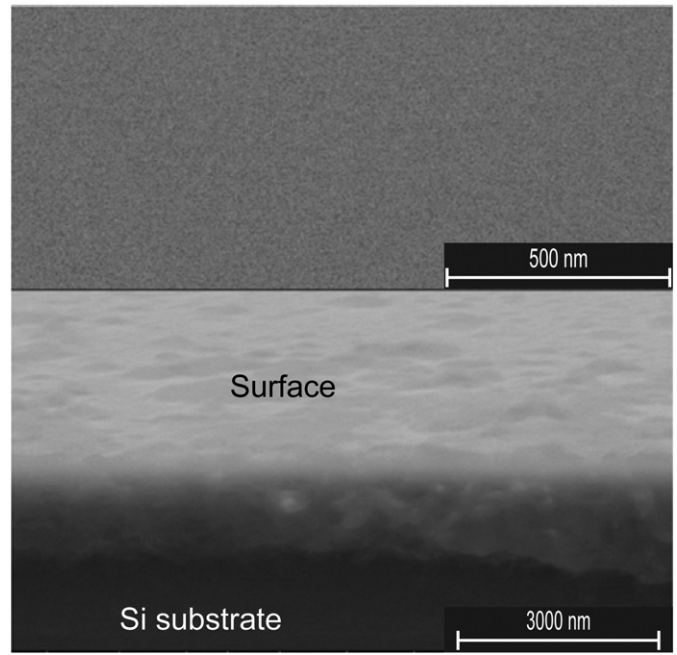


Fig. 6. A surface (top) and cross sectional (bottom) SEM image of a LiPON sample deposited under the best settings (150 W and 0.03 Pa). No crystalline structure was found in the surface.

1 Pa (200 W). As expected, the increase of the room temperature results in higher ionic conductivities. The depositions were done with two controlled parameters: the pressure inside the deposition chamber and the power applied by the RF source of the sputtering system to the Li₃PO₄ target (which would result in different deposition rates). The measurements allow the observation of the following: the ionic conductivity increases with decrease of deposition pressure and with decrease of RF-power of the sputtering source. Moreover, ionic conductivity increases as deposition rate decreases, due to the decrease of pressure and RF-power. As expected, the measurements also showed that an increased room temperature results in a better ionic conductivity.

A typical X-ray diffraction pattern (XRD Bruker, model D8 Discover, copper source of 40 kV and 40 mA, beam wavelength of 1.54 Å

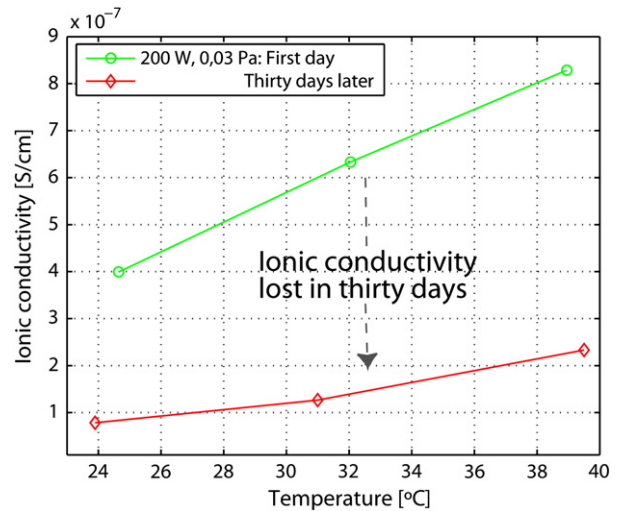


Fig. 7. Ionic conductivity measurement of the LiPON film as deposited and after 30 days of exposure to the atmosphere.

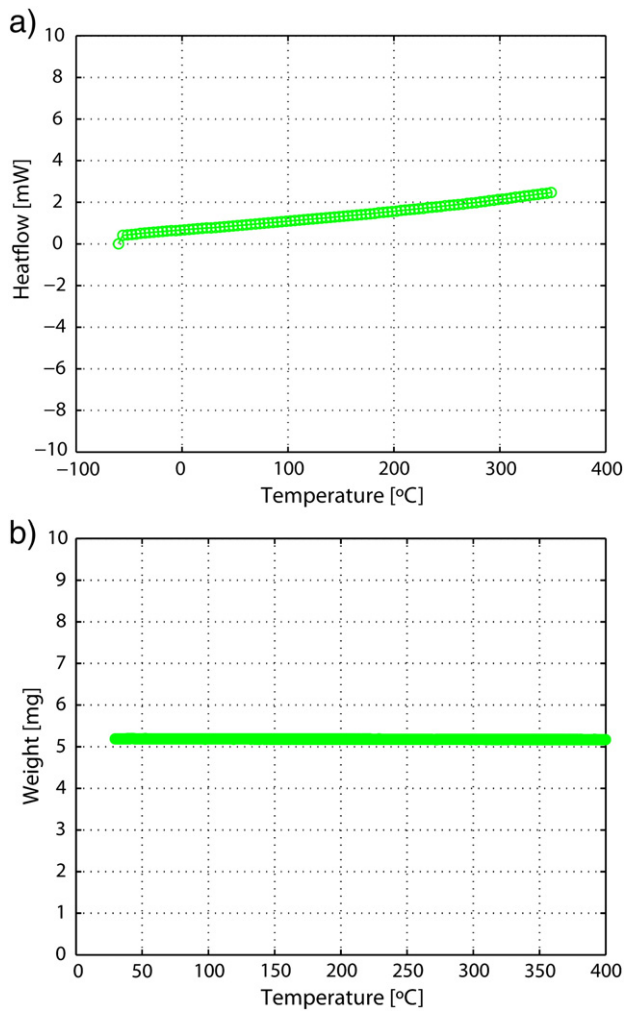


Fig. 8. a) Heatflow (mW) of the LiPON film as a function of temperature during DSC analysis. b) Weight of the LiPON film as a function of temperature during TGA analysis.

and theta/2theta configuration, also called Bragg–Brentano configuration) of Li_3PO_4 is shown in Fig. 5. The XRD of the sputtered LiPON film, in a glass substrate is also shown in Fig. 5. Despite the very intense diffraction peaks of Li_3PO_4 sputtering target, the LiPON films deposited

at N_2 atmosphere are amorphous. Fig. 6 is a surface SEM (NanoSEM-FEI Nova 200 (FEG/SEM)) of a lithium phosphorous oxynitride sample deposited under the best settings (150 W and 0.03 Pa). The ionic conductivity of sample 1 (200 W, 0.03 Pa) was also measured after being exposed to the ambient atmosphere for a month. Fig. 7 shows the ionic conductivity of the film as deposited and after exposure to atmosphere (temperature of 25 °C and humidity of 60%) in 30 days. It was concluded that the ionic conductivity decreased considerably, but the behavior with temperature remained.

The thermal stability of the LiPON films was also measured by Differential Scanning Calorimetry (DSC) and Thermogravimetric analysis (TGA) techniques. The DSC scans were performed in Ar atmosphere using a Mettler Toledo, DSC821 at a constant heating rate of $10\text{ °C}\cdot\text{min}^{-1}$. The weight of each DSC pan with the sample was found to be constant before and after the DSC measurements, indicating that there was no leakage during the experiments. The results in Fig. 8, from DSC (A) and TGA (B) analyses, show that the LiPON is stable when subjected to temperatures up to 400 °C. Finally, Table 2 compares the ionic conductivity of the lithium phosphorous oxynitride films with the measures taken from the related state-of-the-art [4,10,11,15–20]. The lithium phosphorous oxynitride films presented in this paper were shown to be between the highest ionic conductivity when compared with the most recent work done by peers.

4. Conclusions

This paper presented lithium phosphorous oxynitride (LiPON) films, deposited by RF reactive sputtering, with improved characteristics. The highest ionic conductivity ($10^{-6}\text{ S}\cdot\text{cm}^{-1}$) was measured at a room temperature of 35 °C on a LiPON sample obtained from a deposition at 20 sccm of nitrogen (N_2) with a pressure of 0.03 Pa and with an RF applied power of 150 W. The ionic conductivity of the deposited films of LiPON was between the highest presented by the best state-of-the-art [4,10,11,15–20]. XRD and SEM analyses show an amorphous structure for the best sample. TGA and DSC analysis proved stability of the LiPON film at temperatures up to 400 °C. The target application of lithium phosphorous oxynitride films is in solid-state batteries.

Acknowledgments

This work was financially supported by FCT funds with the project PTDC/EEA-ELC/114713/2009 and with first author scholarship SFRH/BD/78217/2011.

Table 2
Ionic conductivity comparison of LiPON films with the related state-of-the-art [4,10,11,15–20].

Reference	RF sputtering conditions of LiPON deposition (RF power, pressure, N_2 flow)	Material for ionic conductivity measurement	Ionic conductivity temperature measurement (°C)	Ionic conductivity [$\text{S}\cdot\text{cm}^{-1}$]
This work	150 W, 3×10^{-2} Pa, 20 sccm	LiPON	35	10^{-6}
W.C. West et al. [16]	Not available, except that Li_3PO_4 target in N_2	LiPON	25,5	5.6×10^{-7}
E. Jeong et al. [17]	Not available, except that $V_{\text{bias(RF)}}\in[-100, -60]\text{V}$	LiPON	Not available	1.16×10^{-6}
H.Y. Park et al. [15]	180 W \times 2, 6.7×10^{-1} Pa, N_2 flow N/A	LiPON	Not available	9.1×10^{-7}
J. M. Lee et al. [10]	90 W, 0.7 Å s^{-1} , 8×10^{-1} Pa, 42 sccm	LiPON/lithium lanthanum titanate/LiPON	Room temperature	2.5×10^{-7}
H.U. Zongqian et al. [18]	$5.5\text{ W}\cdot\text{cm}^{-2}$ (density), 1.5 Pa, N_2 flow N/A	LiPON	Room temperature	3.3×10^{-6}
T. Pichonat et al. [19]	$3.7\text{ W}\cdot\text{cm}^{-2}$ (density), 0.6 Pa, N_2 flow N/A	LiPON	Room temperature	6.0×10^{-7}
S. H. Jee et al. [11]	70 W, 6.7×10^{-1} Pa, N_2 flow N/A	LiPON/lithium phosphorous tungsten oxynitride/LiPON	Room temperature	1.5×10^{-7}
C. S. Nimisha et al. [20]	$3\text{ W}\cdot\text{cm}^{-2}$ (density), 10^{-4} Pa, 30 sccm	LiPON	Room temperature	1.1×10^{-6}
B. Fleutot et al. [4]	$2.0\text{ W}\cdot\text{cm}^{-2}$ (density), 1 Pa, 40 sccm	LiPON	Room temperature	7.2×10^{-6}

References

- [1] M. Armand, J.-M. Tarascon, *Nature* 451 (2008) 652.
- [2] A. Patil, V. Patil, D.W. Shin, J.-W. Choi, D.-S. Paik, S.-J. Yoon, *Mater. Res. Bull.* 43 (2008) 1913.
- [3] H. Lhermet, C. Condemine, M. Plissonnier, R. Salot, P. Audebert, M. Rosset, *IEEE J. Solid State Circuits* 43 (2008) 246.
- [4] B. Fleutot, B. Pecquenard, F. Le Cras, B. Delis, H. Martinez, L. Dupont, D. Guy-Bouyssou, *J. Power Sources* 196 (2012) 10289.
- [5] N.J. Dudney, *Mater. Sci. Eng. B* 116 (2005) 245.
- [6] Y.G. Kim, H.N.G. Wadley, *J. Vac. Sci. Technol. A* 26 (2008) 174.
- [7] J.B. Bates, N.J. Dudney, G.R. Gruzalski, R.A. Zuhr, A. Choudhury, C.F. Luck, J.D. Robertson, *J. Power Sources* 43 (1993) 103.
- [8] J.B. Bates, X. Yu, *J. Vac. Sci. Technol. A* 14 (1996) 34.
- [9] S. Zhao, Z. Fu, Q. Qin, *Thin Solid Films* 415 (2002) 108.
- [10] J.M. Lee, S.H. Kim, Y. Tak, Y.S. Yoon, *J. Power Sources* 163 (2006) 173.
- [11] S.H. Jee, M.-J. Lee, H.S. Ahn, D.-J. Kim, J.W. Choi, S.J. Yoon, S.C. Nam, S.H. Kim, Y.S. Yoon, *Solid State Ionics* 181 (2010) 902.
- [12] C. Li, B. Zhang, Z. Fu, *Thin Solid Films* 515 (2006) 1886.
- [13] L. Meda, E.E. Maxie, *Thin Solid Films* 520 (2012) 1799.
- [14] Y. Hamon, A. Douarda, F. Sabarya, C. Marcela, P. Vinatierb, B. Pecquenardb, A. Levasseur, *Solid State Ionics* 177 (2006) 257.
- [15] H.Y. Park, S.C. Nam, Y.C. Lim, K.G. Choi, K.C. Lee, G.B. Park, S.-R. Lee, H.P. Kim, S.B. Cho, *J. Electroceram.* (2006) 1023.
- [16] W.C. West, J.F. Whitacre, J.R. Lim, *J. Power Sources* 126 (2004) 134.
- [17] E. Jeong, C. Hong, Y. Tak, S.C. Nam, S. Cho, *J. Power Sources* 159 (2006) 223.
- [18] H.U. Zongqian, L.I. Dezhan, Xie Kai, *Bull. Mater. Sci.* 31 (2008) 681.
- [19] T. Pichonat, C. Lethien, N. Tiercelin, S. Godey, E. Pichonat, P. Roussel, M. Colmont, P.A. Rolland, *Mater. Chem. Phys.* 123 (2010) 231.
- [20] C.S. Nimisha, K.Y. Rao, G. Venkatesh, G.M. Rao, N. Munichandraiah, *Thin Solid Films* 519 (2011) 3401.